Inorganic Chemistry

Article

pubs.acs.org/IC

Spin Crossover Iron(II) Coordination Polymer Chains: Syntheses, Structures, and Magnetic Characterizations of $[Fe(aqin)_2(\mu_2\text{-}M(CN)_4)]$ (M = Ni(II), Pt(II), aqin = Quinolin-8-amine)

Fatima Setifi,[†,‡] Eric Milin,[†] Catherine Charles,[†] Franck Thétiot,[†] Smail Triki,*[,†] and Carlos J. Gómez-García[§]

[†]UMR CNRS 6521, Chimie, Electrochimie Moléculaires, Chimie Analytique, Université de Bretagne Occidentale, BP 809, 29285 Brest Cedex, France

[‡]Laboratoire de Chimie, Ingénierie Moléculaire et Nanostructures (LCIMN), Université Ferhat Abbas de Sétif, 19000 Sétif, Algeria

[§]Instituto de Ciencia Molecular (ICMol), Parque Científico, Universidad de Valencia, C/Catedrático José Beltrán, 2, 46980 Paterna, Valencia, Spain

Supporting Information

ABSTRACT: New Fe(II) coordination polymeric neutral chains of formula $[Fe(aqin)_2(\mu_2\text{-}M(CN)_4)]$ (M = Ni^{II} (**1**) and Pt^{II} (**2**)) (aqin = Quinolin-8-amine) have been synthesized and characterized by infrared spectroscopy, X-ray diffraction, and magnetic measurements. The crystal structure determinations of **1**−**2** reveal in both cases a one-dimensional structure in which the planar $[M(CN)_4]^{2-}$ (M = Ni^{II} (**1**) and Pt^{II} (**2**)) anion acts as a μ_2-bridging ligand, and the two aqin molecules as chelating coligands. Examination of the intermolecular contacts in the two compounds reveals that the main contacts are ascribed to hydrogen bonding interactions involving the amine groups of the aqin chelating ligands and the nitrogen atoms of the two non bridging CN groups of the $[M(CN)_4]^{2-}$ (M = Ni^{II} (**1**) and Pt^{II} (**2**)) anion. The average values of the six Fe−N distances observed respectively at room temperature (293 K) and low temperature (120 K), that is, 2.142(3) and 2.035(2) Å for **1**, and 2.178(3) and 1.990(2) Å for **2**, and the thermal variation of the cell parameters (performed on **2**) are indicative of the presence of an abrupt *HS-LS* spin crossover (*SCO*) transition in both compounds. The thermal dependence of the product of the molar magnetic susceptibility times the temperature ($\chi_m T$), in cooling and warming modes, confirms the *SCO* behavior at about 145 and 133 K in **1** and **2**, respectively, and reveals the presence of a small thermal hysteresis of about 2 K for each compound.

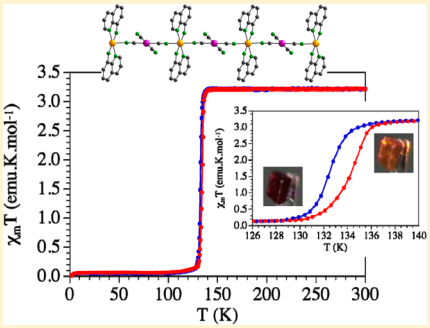

INTRODUCTION

The design of new coordination complexes exhibiting the spin crossover phenomenon (*SCO*) is one of the most relevant challenges in the field of magnetic molecular materials.[1−9] The *SCO* systems relate to the pseudo-octahedral d^4-d^7 transition metal complexes for which the high spin (*HS*) and the low spin (*LS*) electron configurations can be reversibly switched by external stimuli such as temperature, pressure, magnetic field, or light irradiation.[5−20] Nevertheless, the primary investigated systems to date remain those based on Fe(II) (d^6 configuration), for which a paramagnetic-diamagnetic transition from the *HS* (S = 2) state to the *LS* (S = 0) state is observed. Up to now, most of the reported *SCO* Fe(II)-based examples refer to mononuclear compounds.[21−28] In such discrete systems, the intermolecular interactions (π-stacking, hydrogen bonding, and van der Waals interactions), which generate the supramolecular architecture in the solid state, play a crucial role in the information transmission of the magneto-elastic cooperative effects at the origin of the magnetic bistability. However, the non covalent character of those contacts hardens the anticipated design of the supramolecular organization in the crystal, and consequently makes difficult the tailoring of the *SCO* characteristics.

To better explore the cooperative effect between the active metal ions, a new approach based on the use of neutral suitable bridging ligands, able to create covalent links between the metal centers, has been introduced. The first monodimensional polymeric *SCO* compound, $[Fe(Htrz)_2(trz)](BF_4)$ (trz^- = 1,2,4-triazolate anion) was reported by Haasnoot and co-workers in 1977; it exhibits successfully a large thermal hysteresis.[29] Similarly, the use of substituted 1,2,4-triazole ligands led to other one-dimensional (1D) *SCO* polymers for which some of them exhibit cooperativity at high temperature.[30] In parallel, the extension of such polymeric approach to poly-N-donating heterocyclic ligands and to the bis(azolyl)-alkanes resulted in the preparation of several iron(II) *SCO* coordination polymers exhibiting rich and fascinating structural features ranging from 1D to three-dimensional (3D) networks, and various magnetic behaviors.[31−35]

Received: July 4, 2013
Published: December 23, 2013

   dx.doi.org/10.1021/ic401721x | *Inorg. Chem.* 2014, 53, 97−104

Table 1. Crystal Data and Structural Refinement Parameters for Compounds $[Fe(aqin)_2(\mu_2\text{-}M(CN)_4)]$; M = Ni^{II} (1) and Pt^{II} (2)

	1		2	
temperature/K	293(2)	120(2)	293(2)	120(2)
[a]empirical formula	$C_{22}H_{16}N_8FeNi$		$C_{22}H_{16}N_8FePt$	
formula weight	506.99		643.37	
wavelength/Å	0.71073		0.71073 Å	
crystal system	monoclinic		monoclinic	
space group	$P2_1/c$		$P2_1/c$	
a/Å	9.1819(6)	9.0033(5)	9.3073(3)	9.0290(2)
b/Å	12.0719(7)	12.0053(6)	12.1228(4)	12.0904(3)
c/Å	9.7282(5)	9.6117(5)	9.9073(3)	9.8107(3)
β/deg	100.258(6)	100.043(6)	101.670(4)	101.124(3)
volume/Å^3	1061.07(11)	1022.98(9)	1094.74(6)	1050.86(5)
Z	2	2	2	2
D_{calc}/g.cm^{-3}	1.587	1.646	1.952	2.033
abs. coef./mm^{-1}	1.598	1.658	7.072	7.367
$F(000)$	516	516	616	616
crystal size/mm^3	0.16 × 0.08 × 0.05	0.13 × 0.11 × 0.04	0.16 × 0.15 × 0.08	0.16 × 0.15 × 0.08
2θ range/deg	6.56−63.30	6.66−60.00	6.42−60.00	6.56−60.00
refl. collected	10548	7201	10604	10188
unique refl./R_{int}	3324/0.0785	2884/0.0340	3174/0.0330	3057/0.0230
data/restr./N_v	1273/0/148	1571/0/148	2017/0/148	2094/0/148
[b]R1/[c] wR2	0.0423/0.0732	0.0385/0.0984	0.0226/0.0494	0.0186/0.0480
[d]GoF	0.906	0.910	0.973	1.125
$\Delta\rho_{max/min}$ (e Å^{-3})	+0.543/−0.376	+1.319/−0.337	+0.890/−0.351	+1.371/−0.442

[a]The asymmetric unit contains 0.5 of the chemical formula. [b]$R1 = \sum||F_o| - |F_c||/\sum|F_o|$. [c]$wR2 = \{\sum[w(F_o^2 - F_c^2)^2]/\sum[w(F_o^2)^2]\}^{1/2}$. [d]$GoF = \{\sum[w(F_o^2 - F_c^2)^2]/(N_{obs} - N_{var.})\}^{1/2}$.

However, the limited number of potentially appropriate bridging ligands slows down the emergence of extended polymeric systems exhibiting covalent links between the metal active centers. In this context, we have noticeably extended, in recent years, this polymeric approach to the highly conjugated cyanocarbanion ligands involving several potentially donating nitrogen atoms.[36] This led us to the first *SCO* iron(II) molecular neutral chain $[Fe(abpt)_2(tcpd)]$ ($(tcpd)^{2-}$ = (C[C-$(CN)_2]_3)^{2-}$ = 2-dicyanomethylene-1,1,3,3-tetracyanopropanediide anion; abpt = 4-amino-3,5-bis(pyridin-2-yl)-1,2,4-triazole) involving an anion as bridging ligand.[37] In our ongoing work on innovative potentially bridging ligands appropriate for the design of novel *SCO* polymeric systems, we have reported recently two new polymeric chains $[Fe(abpt)_2(M(CN)_4)]$ (M = Ni^{II}, Pt^{II}) involving more rigid anionic bridging ligands.[38] However, these 1D compounds display *SCO* transitions above room temperature, making it difficult to reach any structural and electronic informations on the *HS* state. Thus, with the purpose to better control the transition temperature in such systems involving inorganic planar anions and more distinctly to shift the *SCO* transition below room temperature, we have substituted abpt ligand by other chelating ligands such as the quinolin-8-amine (aqin). This chelating ligand is expected to display lower crystal field energy than the abpt ligand since the discrete $[Fe(abpt)_2(dca)_2]$ complex shows a *SCO* transition at $T_{1/2}$ of 86 K,[39a] while the corresponding aqin discrete complex ($[Fe(aqin)_2(dca)_2]$) is paramagnetic and does not exhibit any *SCO* transition.[39b] We report herein the syntheses and the full structural characterizations including thermal variation of the crystallographic structural data, and magnetic properties of two new *SCO* Fe(II) coordination polymer chains of formula $[Fe(aqin)_2(\mu_2\text{-}M(CN)_4)]$ (M = Ni^{II} (**1**) and Pt^{II} (**2**)) involving tetracyanometallate anions as bridging ligands. Note that this study can be viewed as an extension of large series employing these planar anions or other parent cyano anions such as $[M(CN)_2]^-$ (M = Ag^I, Au^I) to design *SCO* materials exhibiting multidimensional networks including the 3D Hofmann-like Networks.[12,40]

EXPERIMENTAL SECTION

General Remarks. All reactions were carried out under aerobic conditions. The starting materials and solvents were purchased from commercial sources (analytical reagent grade) and used without further purification.

Syntheses of $[Fe(aqin)_2(\mu_2\text{-}M(CN)_4)]$ (M = Ni^{II} (1) and Pt^{II} (2)). An ethanolic solution (5 mL) of aqin (0.5 mmol, 72.08 mg) was added progressively, under continuous stirring, to an aqueous solution (10 mL) of $Fe(BF_4)_2{\cdot}6H_2O$ (0.25 mmol, 84.39 mg). The mixture was stirred at room temperature for 15 min and then an aqueous solution (10 mL) of $K_2[M(CN)_4]$ (for M = Ni^{II}: 0.25 mmol, 60.25 mg; for M = Pt^{II}: 0.25 mmol, 94.34 mg) was added dropwise. The resulting orange precipitate was filtered off, washed with cold water and ethanol, and dried. Yield: 92.6 mg, 73.0% for **1** and 122.8 mg, 76.3% for **2**. For **1**: *Anal.* Calc. (%) for $C_{22}H_{16}FeN_8Ni$: C, 52.1; H, 3.2; N, 22.1. Found: C, 52.3; H, 3.3; N, 21.9. IR (cm^{-1}): 3278(m), 3183(m), 3131(m), 2140(s), 2120(s), 1626(m), 1579(s), 1503 (s), 1471(m), 1424(w), 1400(m), 1375(m), 1320(m), 1223(w), 1203(w), 1173(w), 1134(m), 1103(m) 1071(m), 1053(m), 1026(s), 826(s), 789(s), 772 (s), 717(m), 633(m), 581(m), 520(m), 602(w), 583(w), 555(w), 524(w), 436(s), 420(s). For **2**: *Anal.* Calc. (%) for $C_{22}H_{16}FeN_8Pt$: C, 41.1; H, 2.5; N, 17.4. Found: C, 41.5; H, 2.4; N, 17.6. IR (cm^{-1}): 3283(m), 3181(m), 3130(m), 2146(s), 2131(s), 1625(m), 1578(m), 1502 (s), 1470(m), 1397(w), 1372(w), 1319(m), 1133(w), 1099(w), 1069(m), 1050(s), 1024(s), 827(s), 789(s), 772(s), 714(m), 631(m), 581(m), 555(m), 525(m), 498(m), 470(m).

Single Crystal Preparation of $[Fe(aqin)_2(\mu_2\text{-}M(CN)_4)]$ (M = Ni^{II} (1) and Pt^{II} (2)). Single-crystals of compounds **1**−**2** were synthesized using a silica gel diffusion technique in a straight tube. The gel phase was obtained by addition of tetramethoxysilane (1 mL) to an aqueous solution (9 mL) of $K_2[M(CN)_4]$ (0.45 mmol; 108.4 mg for **1** and 169.8 mg for **2**) with stirring; the gel was formed from the resulting

dx.doi.org/10.1021/ic401721x | *Inorg. Chem.* 2014, 53, 97−104

solution left standing for 6 h. Then, two aqueous solutions (6 mL) of $Fe(SO_4)\cdot 7H_2O$ (0.15 mmol, 41.7 mg) and aqin ligand (0.33 mmol, 47.6 mg) were prepared and carefully layered onto the respective gels. Single-crystals of compounds **1** (dark orange) and **2** (orange), suitable for X-ray analyses, were formed within two weeks. As expected, the IR data for single crystals of both compounds are similar to those observed for the corresponding powders described above.

X-ray Crystallography. Crystallographic studies of the two derivatives (**1**–**2**) were performed at 293 and 120 K, using an Oxford Diffraction Xcalibur κ-CCD diffractometer equipped with a graphite monochromated Mo Kα radiation (λ = 0.71073 Å). The full sphere data collections were performed using 1.0° ω-scans with an exposure time of 150 and 200 s per frame for **1**, 60 and 80 s per frame for **2** at 293 and 120 K, respectively. Data collection and data reduction were done with the CRYSALIS-CCD and CRYSALIS-RED programs on the full set of data.[41] The crystal structures were solved by direct methods and successive Fourier difference syntheses, and were refined on F^2 by weighted anisotropic full-matrix least-squares methods.[42] All non-hydrogen atoms were refined anisotropically, while the hydrogen atoms were calculated and therefore included as isotropic fixed contributors to F_c. All other calculations were performed with standard procedures (WINGX).[43] Crystal data, structure refinement and collection parameters are listed in Table 1. The room-temperature X-ray powder diffraction spectra (XRPD) were recorded on a PANalytical Empyrean X-ray powder diffractometer at 45 kV, 40 mA with a Cu-target tube.

Physical Measurements. Infrared spectra were recorded in the range 4000–200 cm^{-1} on a FT-IR BRUKER ATR VERTEX70 Spectrometer. Diffraction analyses were performed using an Oxford Diffraction Xcalibur κ-CCD diffractometer. Variable temperature magnetic susceptibility measurements were carried out in the temperature range 2–300 K in cooling and warming scans with an applied magnetic field of 0.5 T on polycrystalline samples obtained grinding single crystals of compounds **1** and **2** (with masses of 6.805 and 3.600 mg, respectively) with a Quantum Design MPMS-XL-5 SQUID magnetometer. The susceptibility data were corrected for the sample holders previously measured under the same conditions, and for the diamagnetic contributions as deduced by using Pascal's constant tables ($\chi_{dia} = -245.36 \times 10^{-6}$ and -273.36×10^{-6} emu.mol^{-1} for **1** and **2**, respectively).[44] The magnetic measurements were performed with different cooling and warming rates in the range 0.5–5 K/min. The results obtained, within experimental error, were independent of the rate. Elemental analyses were performed at the "Service de microanalyse", CNRS, 91198 Gif-sur-Yvette, France.

RESULTS AND DISCUSSION

Single-crystals of compounds **1** and **2** were synthesized using a silica gel diffusion since the direct mixture of the precursors yielded microcrystalline powders in all cases. Single-crystals of compounds **1** (dark orange) and **2** (orange), suitable for X-ray analysis, were formed within two weeks. The room-temperature XRPD of compound **1** has been performed to confirm that the sample used for magnetic and infrared measurements is effectively identical to the corresponding single crystals used for X-ray structure study (see Supporting Information, Figure S1). The IR spectra of compounds **1** and **2** show two characteristic $\nu_{(CN)}$ bands (2140(s), 2120(s) for **1** and 2146(s), 2131(s) for **2**) which are distinct from the stretching vibration modes observed in $K_2[M(CN)_4]\cdot xH_2O$ ($M = Ni^{II}$ and Pt^{II}).[45] These values can be respectively assigned to the presence of bridging and terminal CN groups, in agreement with the bridging coordination mode of the $[M(CN)_4]^{2-}$ anions in both compounds.

The crystal structures of compounds **1**–**2** were performed at room temperature (293 K) and at 120 K. The unit cell parameters, crystal and refinement data are summarized in Table 1. Selected bond lengths and angles for the iron(II) coordination sphere, including distortion parameters, are summarized in Table 2. The following general structural

Table 2. Selected Bond Lengths (Å), Bond Angles, and Distortion Parameters (deg) of the Fe(II) Coordination Spheres for Compounds 1–2[a]

	1 (M = Ni^{II})		**2** (M = Pt^{II})	
T/K	293	120	293	120
Fe–N1	2.131(3)	2.022(2)	2.170(3)	1.989(2)
Fe–N2	2.161(2)	2.071(2)	2.206(3)	2.031(2)
Fe–N3	2.133(3)	2.011(2)	2.157(3)	1.949(2)
⟨Fe–*N*⟩	2.142(3)	2.035(2)	2.178(3)	1.990(2)
N1–Fe–N3	87.41(10)	87.67(10)	87.68(11)	87.46(10)
N1–Fe–$N3^{(i)}$	92.59(10)	92.33(10)	92.32(11)	92.54(10)
N1–Fe–N2	78.88(10)	82.22(9)	77.48(10)	83.02(10)
N1–Fe–$N2^{(i)}$	101.12(10)	97.78(9)	102.52(10)	96.98(10)
N2–Fe–N3	93.14(9)	93.68(9)	92.85(10)	93.98(10)
N2–Fe–$N3^{(i)}$	86.86(9)	86.32(9)	87.15(10)	86.02(10)
[b]Σ	67	55	71	54
[c]Θ	207	154	233	144

[a]Codes of equivalent positions: (i) $-x,-y,1-z$. [b]Σ is the sum of the deviation from 90° of the 12 *cis*-angles of the FeN_6 octahedron.[48] [c]Θ is the sum of the deviation from 60° of the 24 trigonal angles of the projection of the FeN_6 octahedron onto its trigonal faces.[49]

descriptions are specified at 293 K for both compounds. The pertinent structural modifications induced by cooling or warming will be discussed further in the paragraph dealing with structural and magnetic properties relationships. The two compounds are isostructural as the structure is built from one Fe(II) cation, one $[M(CN)_4]^{2-}$ anion (M = Ni^{II}(**1**) and Pt^{II} (**2**)), both located on inversion centers, and one chelating aqin ligand located on a general position. As shown in Figure 1, the Fe(II) ion adopts a distorted FeN_4N_2 octahedral geometry, with four equatorial nitrogen atoms from two aqin chelating ligands (N1, N2, $N1^{(i)}$, and $N2^{(i)}$), and two axial nitrogen atoms (N3 and $N3^{(i)}$) from two equivalent $[M(CN)_4]^{2-}$ ligands. At room temperature, the average values of the six Fe–N distances are 2.142(3) and 2.178(3) Å for **1** and **2**, respectively. The bond lengths and angles of the two $[M(CN)_4]^{2-}$ (M = Ni^{II}, Pt^{II}) anions are similar to those observed in other coordination complexes involving this moiety.[46,47] The trigonal distortion of the octahedral Fe(II) environment is highlighted by the Σ and Θ parameters (see details in Table 2).[48,49]

Indeed, the relatively high values of the Σ and Θ parameters observed for both compounds at room temperature are indicative of the high degree of distortion of the FeN_6 octahedrons, typical of a *HS* coordination sphere. The resulting molecular structures for **1**–**2** can be described as a chain running along the crystallographic [001] direction, in which the planar $[M(CN)_4]^{2-}$ (M = Ni^{II}, Pt^{II}) anion acts as a μ_2-bridging ligand via two nitrogen atoms of two trans cyano groups (Figure 1). Along the neutral chains, the shortest Fe···Fe (Fe···$Fe^{(iii)}$ in Figure 1) and M···M distances (see Figure 1 for M = Pt^{II}) are simply defined by the length of the crystallographic *c* cell parameter (see Table 1). Consequently and as clearly depicted in Figure 1, these intrachain separations (Fe···Fe and M···M, with M = Ni^{II} (**1**) and Pt^{II} (**2**)) impose the shortest Fe···M distance to equal half of the crystallographic *c* cell parameter (4.8641(5) and 4.9536(3) Å at 293 K for **1** and **2**, respectively), in agreement with the linear arrangement of the metal ions along the [001] direction. The crystal packing of **1**–

dx.doi.org/10.1021/ic401721x | *Inorg. Chem.* 2014, 53, 97–104

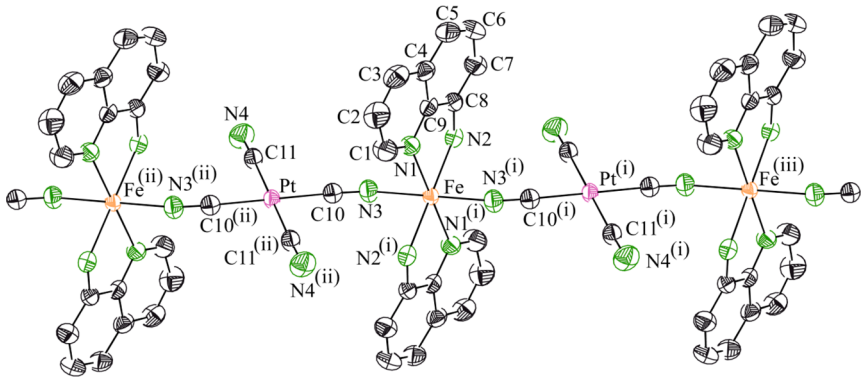

Figure 1. Ortep[50] plot (50% probability ellipsoids) of the 1D neutral structure of **2** at 293 K showing the asymmetric unit, the atom labeling scheme, and the metal ion environment. Codes of equivalent positions: (i) $-x,-y,1-z$; (ii) $-x,-y,-z$; (iii) $x,y,z+1$ (similar figure for the Ni^{II} analogue (**1**)).

2 is generated from the regular chains which are arranged in an eclipsed fashion along the [100] direction, leading to the structural arrangement depicted in Figure 2.

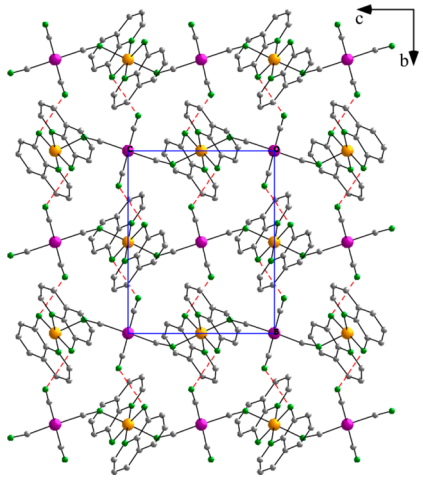

Figure 2. Projection view of the overall molecular structure of compound **2** (similar to **1**) showing the eclipsed packing of the 1D bimetallic coordination polymer along the [100] direction, and the interchain hydrogen bonding (red dashed lines) along the [010] direction.

Careful examination of the intermolecular separations in the two compounds (Figures 2–3 and Table 3) reveals two main types of interchain contacts, both occurring in the [010] direction: (i) hydrogen bonding interactions involving one of the hydrogen atoms of the amine group (N2 and $N2^{(i)}$) of the chelating aqin ligands and the nitrogen atom of the two non bridging CN groups (N4 and $N4^{(ii)}$) from the $[M(CN)_4]^{2-}$ anion of an adjacent chain ($N2\cdots N4^{(b)}$ 3.123(4) and 3.132(4) Å for **1** and **2**, respectively), leading to the structural arrangement depicted in Figure 2 and (ii) the π-stacking interactions between two aqin ligands from two adjacent chains, as shown in Figure 3. The shortest interchain contacts observed for both compounds, as well as their thermal evolution, are gathered in Table 3.

The thermal dependence of the product of the molar magnetic susceptibility per Fe(II) ion times the temperature ($\chi_m T$) is depicted in Figures 4–5. For compound **1**, the $\chi_m T$ value observed at room temperature (300 K) is about 2.65 emu·K·mol^{-1}. This value is significantly lower than the value expected for a hexacoordinated *HS* ($S = 2$, $^5T_{2g}$) Fe(II) ion.

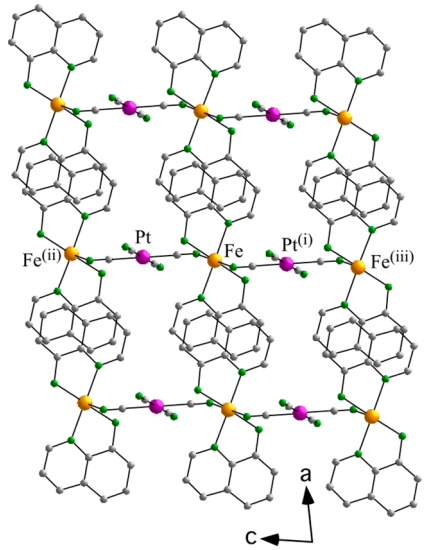

Figure 3. Projection view of **2** (similar to **1**) showing the interchain π-stacking contacts between aqin coligands from adjacent chains. Codes of equivalent positions: (i) $-x,-y,1-z$; (ii) $-x,-y,-z$; (iii) $x,y,z+1$.

This relatively low $\chi_m T$ value indicates the existence, at room temperature, of a fraction of about 20% of Fe(II) ions in the *LS* configuration. It is also noteworthy to indicate that even upon heating the sample above 300 K, the $\chi_m T$ product remains almost constant, and the transition is not fully achieved at 400 K. Upon cooling, the $\chi_m T$ product of **1** decreases gradually, down to a value of about 2.3 emu·K·mol^{-1} at a temperature of about 150 K. Below this temperature, a sharp decrease is observed, indicating the occurrence of an abrupt *HS-LS SCO* transition, with a transition temperature ($T_{1/2}$) of about 145 K. Below 120 K, the $\chi_m T$ value is close to about 0.50 cm^3·K·mol^{-1}, in agreement with the presence of a residual fraction (ca. 15%) of Fe(II) ions in the *HS* configuration. The presence of about 1/5 fraction of Fe(II) centers which remain in the *HS* configuration at low temperatures may be attributed to the presence of defects and vacancies in the chain that lead to the formation of more or less large 1D islands where the *HS* to *LS* transition of one Fe(II) center prevents its neighbors to transit, resulting in a fraction of *HS* Fe(II) centers. The presence of a similar fraction of Fe(II) centers in **1** that remain in the *LS* configuration even at high temperatures (400 K) may be attributed to vacancies or defects in the lattice, or to the possible linkage isomerism of a small fraction of the CN

dx.doi.org/10.1021/ic401721x | *Inorg. Chem.* 2014, 53, 97–104

Table 3. Main Interchain π-Stacking C···C contacts and shortest N···N hydrogen bonding (Å) in 1−2[a]

		1 (M = Ni^{II})		2 (M = Pt^{II})	
		T = 293 K	T = 120 K	T = 293 K	T = 120 K
π-stacking C···C contacts	C3···C7$^{(iv)}$	3.497(1)	3.465(1)	3.505(1)	3.490(1)
	C5···C9$^{(iv)}$	3.567(1)	3.558(1)	3.564(1)	3.588(1)
	C4···C7$^{(iv)}$	3.548(1)	3.483(1)	3.621(1)	3.534(1)
	C5···C8$^{(iv)}$	3.540(1)	3.491(1)	3.628(1)	3.544(1)
	C4···C8$^{(iv)}$	3.643(1)	3.640(1)	3.674(1)	3.718(1)
	C6···C9$^{(iv)}$	3.604(1)	3.561(1)	3.676(1)	3.608(1)
	C4···C6$^{(iv)}$	3.708(1)	3.654(1)	3.762(1)	3.658(1)
N···N H-bonding	N2···N4$^{(v)}$	3.123(4)	3.069(3)	3.132(4)	3.059(4)

[a]Codes of equivalent positions: (iv) 1−x,−y,1−z, (v) x,−1/2−y,1/2+z.

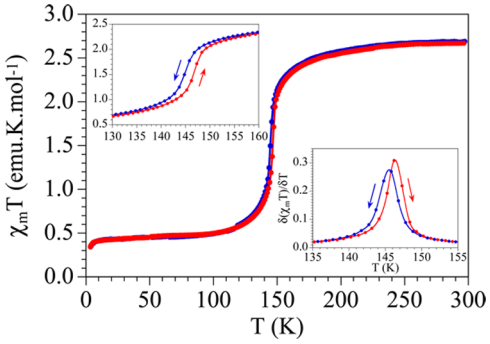

Figure 4. Thermal variation of the $\chi_m T$ product in **1** in the cooling (blue) and warming (red) scans. Left inset shows a zoom of the transition. Right inset shows the thermal variation of the derivative of $\chi_m T$.

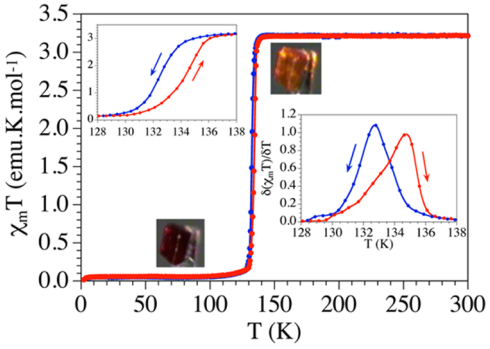

Figure 5. Thermal variation of the $\chi_m T$ product in **2** in the cooling (blue) and warming (red) scans. Left inset shows a zoom of the transition. Right inset shows the thermal variation of the derivative of $\chi_m T$.

bridges. However, this last hypothesis could not be *clear-cut* verified with the IR spectra study since the new bands expected for the small fraction of putative Fe-CN-Ni isomer were not unambiguously detectable, possibly as a consequence of their supposed weak intensity with also the potential masking effect from the more intense bands assigned to the two non bridging and the two bridging CN groups. In addition, there are no structurally characterized examples of Fe^{II}-CN-Ni^{II} linkage isomerism, even if they are known in other CN-bridged systems with Cr^{III} and different M^{II} ions as Fe, Co, and Cu.[51] Interestingly, this CN linkage isomerism would not be expected in the Pt derivative (**2**), in agreement with the much softer character of the Pt(II) ion as compared with the Ni(II) one. Furthermore, the warming mode reveals a very small hysteresis of about 2 K (insets in Figure 4). At very low temperatures, the residual fraction of *HS* Fe(II) ions shows the expected zero field splitting (*ZFS*), leading to a slight decrease of the $\chi_m T$ product, to reach a value of about 0.35 emu·K·mol^{-1} at 2 K.

For the Pt analogue (**2**), the $\chi_m T$ value observed in the high temperature region is about 3.30 emu K mol^{-1}. This value is consistent with a S = 2 *HS* state of the octahedral Fe(II) ions with $g \approx 2.1$. Upon cooling, the $\chi_m T$ product remains constant, down to a temperature of about 134 K. Below this temperature, the sharp decrease on display is indicating the occurrence of an abrupt *HS-LS SCO* transition, as expected from the abrupt color change observed for the single crystals (Figure 5). Below 132 K, the $\chi_m T$ value is close to 0.0 cm^3·K·mol^{-1}, hence revealing the absence of any significant residual fraction of *HS* Fe(II) ions. The warming mode shows a slight thermal hysteresis; indeed, the spin transition temperatures ($T_{1/2}$) for the cooling ($T_{1/2}^{down}$) and warming ($T_{1/2}^{up}$) scans are 132.5 and 134.5 K, respectively, indicating the occurrence, as in **1**, of an about 2 K wide hysteresis loop (see insets Figure 5). The presence of these narrow thermal hysteresis in both compounds can be explained thanks to the existence of weak intermolecular interactions (H-bonds and $\pi-\pi$ stacking in both compounds) described above.

On the basis of the conclusions derived from the magnetic data, the crystal structures have been determined at 293 and 120 K for both compounds, and the temperature dependence measurement of the lattice parameters of a single crystal of **2** was performed in the range 293−100 K. The corresponding structural parameters are depicted in Figures 6−7 and in Table 2. Some of these parameters, such as the average coordination distance ⟨Fe-N⟩ and trigonal distortion parameters Σ and

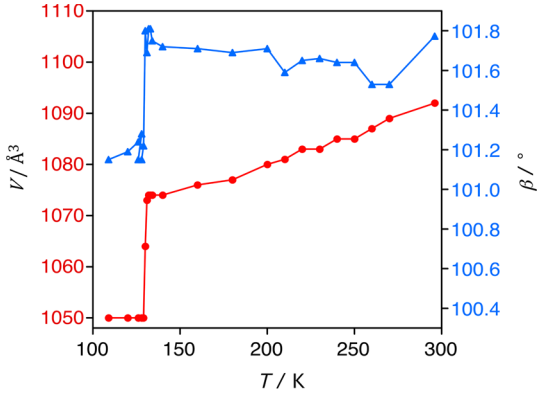

Figure 6. Thermal variation of the unit cell volume (●) and the angular β (▲) parameter in **2** (the blue and red lines are indicated simply to guide the eye).

dx.doi.org/10.1021/ic401721x | Inorg. Chem. 2014, 53, 97−104

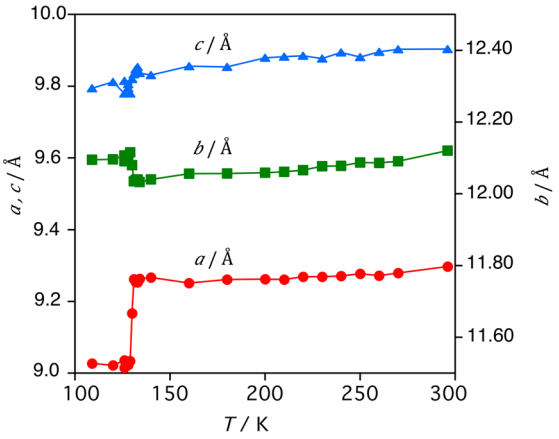

Figure 7. Thermal variations of the lattice parameters of compound **2**; *a* (●), *b* (■), and *c* (▲) parameters revealing the abrupt *SCO* transition, the transition temperature, and the anisotropic contraction of the crystal. The two vertical axis are drawn using the same scale (the blue, green, and red lines are indicated simply to guide the eye).

(previously defined in Table 2), are known to be highly sensitive to the Fe(II) spin configuration, and will thus be used hereafter to assign the spin state on each Fe crystallographic site ($\langle$Fe-*N*$\rangle_{LS}$ ∼ 2.0 Å; $\langle$Fe-*N*$\rangle_{HS}$ ∼ 2.2 Å).[37,46,47]

The thermal variation of the average values of the six Fe−N distances observed for **1**−**2** at room and low temperatures (2.142(3) and 2.035(2) Å for **1**; and 2.178(3) and 1.990(2) Å for **2**, at 293 and 120 K, respectively) reveals strong modifications of the iron coordination spheres in both compounds. For compound **2**, the averaged values observed at 293 and 120 K are in the range of those expected for the *HS* (∼ 2.2 Å) and the *LS* (∼ 2.0 Å) states of the Fe(II) ion, in complete agreement with the corresponding magnetic data aforementioned for this compound. Conversely, the averaged Fe−N value observed at room temperature for **1** (2.142(3) Å) is lower than the value expected for 100% *HS* state of the Fe(II) ions (∼ 2.2 Å), and so in agreement with the presence, at room temperature, of a remaining *LS* fraction of Fe(II) ions of about 19%, and very close to the corresponding value calculated with the magnetic data (ca. 20%). At low temperature (120 K), the averaged Fe−N value for **1** (2.035(2) Å) is significantly higher than the one expected for a complete magnetic transition (∼ 2.0 Å). The latter value suggests the presence of a *HS* fraction of about 17%, again very close to the corresponding value resulting from the analysis of the magnetic data (15%) of **1**.

For both compounds, the trigonal distortion parameters Σ and Θ are significantly reduced from room to low temperatures (for **1**, Σ decreases from 67° to 55° and Θ from 207° to 154° at 293 and 120 K, respectively; while for **2**, Σ is reduced from 71° to 54° and Θ from 233° to 144° at 293 and 120 K, respectively). Owing to the more regular FeN_6 octahedral geometry in the *LS* state, those observations are in line with the presence of a *SCO* transition from *HS* to *LS* in both compounds. Furthermore, the variations of the Σ and Θ parameters are significantly stronger in **2** (17° and 89°, respectively) than in **1** (12° and 53°, respectively), suggesting that the transition is more complete in **2** than in **1** which is in agreement with both magnetic measurements and Fe−N bond lengths arguments. It is also worth to indicate that the modifications of the iron coordination spheres in the two compounds affect more significantly the Fe−N3 bonds running along the chain direction (For **1**: 2.133(3) and 2.011(2) Å at 293 and 120 K respectively, Δ(Fe−N) = 0.122 Å; for **2**: 2.157(3) and 1.949(2) Å at 293 and 120 K respectively, Δ(Fe−N) = 0.208 Å). Interestingly, the significant decrease of the Fe−N3 bond lengths, from room to low temperature, does not affect strongly the shortest Fe···Fe distance along the polymeric chain (Fe-(NC-M-CN)-Fe: 9.7282(5) and 9.6117(5) Å for **1** and 9.9073(3) and 9.8107(3) Å for **2**, at 293 and 120 K, respectively). This result is due to the increase of the Fe−N3−C10 bond angles from room to low temperature (from 145.6(3)° to 151.5(2)° in **1** and from 142.0(3)° to 156.2(2)° in **2**, at 293 and 120 K, respectively), that partially compensate the strong decrease of the Fe−N3 bond lengths and mitigate its effect on the Fe···Fe distances along the molecular chain.

To clearly establish how the crystal and the lattice parameters were affected by the magnetic transition, we have measured the temperature dependence of the lattice parameters of a single crystal of **2** in the range 293−100 K. As can be seen in Figures 6−7, the *a*, *b*, *c* and *β* unit cell parameters, as well as the unit cell volume (*V*), show abrupt decreases at the same temperature than the one obtained from the magnetic data, that is, 132 K. This behavior is typical of *SCO* transitions and, together with the abrupt color change in the single crystal also observed at about 132 K (Figures 5-7), confirms the presence of a *SCO* transition at about 132 K. The unit cell parameters remain relatively constant and do not reveal any significant decrease in the temperature range 293−132 K, that is, before the *SCO* transition. According to the magnetic data (Figure 5), those structural data clearly demonstrate that the single crystal of **2** contracts anisotropically on cooling, since the more significant changes occur essentially along the *a* axis (Figure 7).

■ CONCLUSIONS

In summary, we have reported here the syntheses, the structural characterizations at high and low temperature, the temperature dependence of the lattice parameters, and the magnetic properties of the two isostructural *SCO* Fe(II) molecular neutral chain $[Fe(aqin)_2(M(CN)_4)]$ (M = Ni^{II}(**1**) and Pt^{II} (**2**)). The molecular chain structure of both compounds is generated by the $[M(CN)_4]^{2-}$ moiety acting as a μ_2-bridging ligand via two nitrogen atoms from two trans cyano groups. The X-ray diffraction studies, in the range 293−120 K, show strong modifications of the iron coordination spheres, in agreement with the presence of a *SCO* transition in compounds **1**−**2**; also clearly confirmed by the thermal variation of the $\chi_m T$ product. Additionally, the thermal dependence of the lattice parameters *a*, *b*, *c* and *β*, as well as the unit cell volume (*V*), shows abrupt decreases at the same temperature than the one obtained from the magnetic data, and reveals that the single crystal of **2** contracts anisotropically on cooling, since the more significant changes occur essentially along the *a* axis. From a synthetic point of view, this study confirms the ability of the polycyanometallate anions to generate novel *SCO* complexes exhibiting original extended arrangements. An additional advantage of the use of such anions resides in their structural similarity with their parent analogues, such as the paramagnetic hexacyanometallate anions. Thus, besides their high ability to coordinate and bridge transition metal ions, these paramagnetic anions can transmit magnetic coupling between the metal active centers. Accordingly, attempts to prepare multidimensional bimetallic architectures combining *SCO* behavior and magnetic interactions using such magnetic polybridging anions are underway.

dx.doi.org/10.1021/ic401721x | *Inorg. Chem.* 2014, 53, 97−104

■ ASSOCIATED CONTENT

Supporting Information

X-ray crystallographic data in CIF format (CCDC numbers: 938438 and 931126 for **1** at 293 and 120 K, respectively; 924207 and 924208 for **2** at 293 and 120 K, respectively) and observed and calculated X-ray powder diffraction patterns for (**1**). This material is available free of charge via the Internet at http://pubs.acs.org.

■ AUTHOR INFORMATION

Corresponding Author

*E-mail: smail.triki@univ-brest.fr. Phone: +33 298 016 146. Fax: +33 298 017 001.

Notes

The authors declare no competing financial interest.

■ ACKNOWLEDGMENTS

The authors acknowledge the CNRS ("Centre National de la Recherche Scientifique"), the Brest University, the French "Ministère de la Recherche" and "Ministère des Affaires Etrangères et Européennes" (PHC Maghreb project No. 13MAG08), the "Agence Nationale de la Recherche" (ANR project BISTA-MAT: ANR-12-BS07-0030-01), the "Spanish Ministerio de Economía y Competitividad" (Project CTQ2011-26507), and the "Generalitat Valenciana" (projects Prometeo and ISIC).

■ REFERENCES

(1) Gütlich, P., Goodwin, H. A., Eds.; Spin Crossover in Transition Metal Compounds I-III. In *Topics in Current Chemistry*; Springer Verlag: Berlin, Germany, 2004; Vols. *233*−*235*.
(2) Gamez, P.; Costa, J. S.; Quesada, M.; Aromí, G. *Dalton Trans.* **2009**, 7845−7853 and references therein.
(3) Létard, J.-F.; Guionneau, P.; Goux-Capes, L. *Top. Curr. Chem.* **2004**, *235*, 221−249.
(4) Cobo, S.; Molnár, G.; Real, J. A.; Bousseksou, A. *Angew. Chem., Int. Ed.* **2006**, *45*, 5786−5789.
(5) Olguin, J.; Brooker, S. *Coord. Chem. Rev.* **2011**, *255*, 203−240.
(6) Halcrow, M. A. *Chem. Soc. Rev.* **2011**, *40*, 4119−4142.
(7) Prins, F.; Monrabal-Capilla, M.; Osorio, E. A.; Coronado, E.; J. van der Zant, H. S. *Adv. Mater.* **2011**, *23*, 1545−1549.
(8) Muñoz-Lara, F. J.; Arcís-Castillo, Z.; Muñoz, M.-C.; Rodríguez-Velamazán, J.-A.; Gaspar, A.-B.; Real, J.-A. *Inorg. Chem.* **2012**, *51*, 11126−11132.
(9) Gütlich, P.; Gaspar, A.-B.; Garcia, Y. *Beilstein J. Org. Chem.* **2013**, *9*, 342−391.
(10) Decurtins, S.; Gütlich, P.; Köhler, C. P.; Spiering, H.; Hauser, A. *Chem. Phys. Lett.* **1984**, *105*, 1−4.
(11) Létard, J.-F. *J. Mater. Chem.* **2006**, *16*, 2550−2559.
(12) (a) Rodríguez-Velamazán, J. A.; Castro, M.; Palacios, E.; Burriel, R.; Kitazawa, T.; Kawasaki, T. *J. Phys. Chem. B* **2007**, *111*, 1256−1261. (b) Niel, V.; Muñoz, M. C.; Gaspar, A. B.; Galet, A.; Levchenko, G.; Real, J. A. *Chem.—Eur. J.* **2002**, *8*, 2446−2453. (c) Kosone, T.; Kanadani, C.; Saito, T.; Kitazawa, T. *Polyhedron* **2009**, *28*, 1991−1995.
(13) Garcia, Y.; Gütlich, P. *Top. Curr. Chem.* **2004**, *234*, 49−62.
(14) Morgan, G. G.; Murnaghan, K. D.; Müller-Bunz, H.; McKee, V.; Harding, C. J. *Angew. Chem., Int. Ed.* **2006**, *45*, 7192−7195.
(15) Sim, P. G.; Sinn, E. *J. Am. Chem. Soc.* **1981**, *103*, 241−243.
(16) Halepoto, D. M.; Holt, D. G. L.; Larkworthy, L. F.; Leigh, G. L.; Povey, D. C.; Smith, G .W. *J. Chem. Soc., Chem. Commun.* **1989**, 1322−1323.
(17) van Konigsbruggen, P. J.; Maeda, Y.; Oshio, H. *Top. Curr. Chem.* **2004**, *233*, 259−324.
(18) Costes, J.-P.; Dahan, F.; Laurent, J.-P. *Inorg. Chem.* **1990**, *29*, 2448−2452.
(19) Ishikawa, R.; Matsumoto, K.; Onishi, K.; Kubo, T.; Fuyuhiro, A.; Hayami, S.; Inoue, K.; Kaizaki, S.; Kawata, S. *Chem. Lett.* **2009**, *38*, 620−621.
(20) Hayami, S.; Moriyama, R.; Shigeyoshi, Y.; Kawajiri, R.; Mitani, T.; Akita, M.; Inoue, K.; Maeda, Y. *Inorg. Chem.* **2005**, *44*, 7295−7297.
(21) Galet, A.; Gaspar, A. B.; Muñoz, M. C.; Levchenko, G.; Real, J. A. *Inorg. Chem.* **2006**, *45*, 9670−9679.
(22) Dupouy, G.; Marchivie, M.; Triki, S.; Sala-Pala, J.; Salaün, J.-Y.; Gómez-García, C. J.; Guionneau, P. *Inorg. Chem.* **2008**, *47*, 8921−8931.
(23) Sheu, C.-F.; Pillet, S.; Lin, Y.-C.; Chen, S.-M.; Hsu, I.-J.; Lecomte, C.; Wang, Y. *Inorg. Chem.* **2008**, *47*, 10866−10874.
(24) El Hajj, F.; Sebki, G.; Patinec, V.; Marchivie, M.; Triki, S.; Handel, H.; Yefsah, S.; Tripier, R.; Gómez-García, C. J.; Coronado, E. *Inorg. Chem.* **2009**, *48*, 10416−10423.
(25) Weber, B.; Bauer, W.; Obel, J. *Angew. Chem., Int. Ed.* **2008**, *47*, 10098−10101.
(26) Weber, B.; Kaps, E.; Weigand, J.; Carbonera, C.; Létard, J.-F.; Achterhold, K.; Parak, F.-G. *Inorg. Chem.* **2008**, *47*, 487−496.
(27) Reger, D. L.; Gardinier, J. R.; Elgin, J. D.; Smith, M. D.; Hautot, D.; Long, G. J.; Grandjean, F. *Inorg. Chem.* **2006**, *45*, 8862−8875.
(28) Weber, B.; Jäger, E.-G. *Eur. J. Inorg. Chem.* **2009**, 465−477.
(29) Haasnoot, J. G.; Vos, J. G.; Groeneveld, W. L. *Z. Naturforsch. B* **1977**, *32*, 1421−1430.
(30) (a) Garcia, Y.; van Koningsbruggen, P. J.; Lapouyade, P.; Rabardel, L.; Khan, O.; Wierczorek, M.; Bronisz, R.; Ciunik, Z.; Rudolf, M. F. *C. R. Acad. Sci. Paris IIc* **1998**, *1*, 523. (b) Kahn, O.; Martinez, C. J. *Science* **1998**, *279*, 44−48. (c) Dîrtu, M. M.; Schmit, F.; Naik, A. D.; Rotaru, A.; Marchand-Brynaert, J.; Garcia, Y. *Int. J. Mol. Sci* **2011**, *12*, 5339−5351.
(31) Garcia, Y.; Kahn, O.; Rabardel, L.; Chansou, B.; Salmon, L.; Tuchagues, J.-P. *Inorg. Chem.* **1999**, *38*, 4663−4670. Bronisz, R. *Inorg. Chem.* **2005**, *44*, 4463.
(32) (a) Genre, C.; Jeanneau, E.; Bousseksou, A.; Luneau, D.; Borshch, S. A.; Matouzenko, G. S. *Chem.—Eur. J.* **2008**, *14*, 697−705. (b) Matouzenko, G. S.; Jeanneau, E.; Luneau, D. *New J. Chem.* **2006**, *30*, 1669−1674.
(33) (a) Moliner, N.; Muñoz, M. C.; Létard, S.; Salmon, L.; Tuchagues, J.-P.; Bousseksou, A.; Real, J. A. *Inorg. Chem.* **2002**, *41*, 6997−7005. (b) Matouzenko, G. S.; Perrin, M.; Le Guennic, B.; Genre, C.; Molnár, G.; Bousseksou, A.; Borshch, S. A. *Dalton Trans.* **2007**, 934. (c) Genre, C.; Matouzenko, G. S.; Molnár, G.; Bréfuel, N.; Perrin, M.; Bousseksou, A.; Borshch, S. A. *Chem. Mater.* **2003**, *15*, 550−556.
(34) (a) Real, J. A.; Gaspar, A. B.; Niel, V.; Muñoz, M. C. *Coord. Chem. Rev.* **2003**, *236*, 121−141. (b) Garcia, Y.; Niel, V.; Muñoz, M. C.; Real, J. A. *Top. Curr. Chem.* **2004**, *233*, 229−257.
(35) Murray, K. S.; Kepert, C. J. *Top. Curr. Chem.* **2004**, *233*, 195−228.
(36) Benmansour, S.; Atmani, C.; Setifi, F.; Triki, S.; Marchivie, M.; Gómez-García, C. J. *Coord. Chem. Rev.* **2010**, *254*, 1468−1478.
(37) (a) Dupouy, G.; Marchivie, M.; Triki, S.; Sala-Pala, J.; Gomez-Garcia, C. J.; Pillet, S.; Lecomte, C.; Létard, J.-F. *Chem. Commun.* **2009**, 3404−3406. (b) Dupouy, G.; Triki, S.; Marchivie, M.; Cosquer, N.; Gómez-García, C. J.; Pillet, S.; Bendeif, E.-E.; Lecomte, C.; Asthana, S.; Létard, J.-F. *Inorg. Chem.* **2010**, *49*, 9358−9368.
(38) Setifi, F.; Charles, C.; Houille, S.; Thétiot, F.; Triki, S.; Gómez-García, C. J.; Pillet, S. *Polyhedron* **2013**, *61*, 242−247.
(39) (a) Moliner, N.; Gaspar, A. B.; Muñoz, M. C.; Niel, V.; Cano, J.; Real, J.-A. *Inorg. Chem.* **2001**, *40*, 3986−3991. (b) Setifi, F.; Thétiot, F.; Triki, S.; Gómez-García, C. J. (manuscript in preparation).
(40) (a) Kitazawa, T.; Gomi, Y.; Takahashi, M.; Takeda, M.; Enomoto, M.; Miyazaki, A.; Enoki, T. *J. Mater. Chem.* **1996**, *6*, 119−121. (b) Niel, V.; Martinez-Agudo, J. M.; Muñoz, M. C.; Gaspar, A. B.; Real, J. A. *Inorg. Chem.* **2001**, *40*, 3838−3839. (c) Molnar, G.; Niel, V.; Gaspar, A. B.; Real, J. A.; Zwick, A.; Bousseksou, A.; McGarvey, J. J. *J. Phys. Chem. B* **2002**, *106*, 9701−9707.
(41) *CRYSALIS-CCD 170, CRYSALIS-RED 170*; Oxford-Diffraction: Abingdon, U.K., 2002.

(42) Sheldrick, M. *SHELX97, Program for Crystal Structure Analysis*; University of Göttingen: Göttingen, Germany, 1997.
(43) Farrugia, L. J. *J. Appl. Crystallogr.* **1999**, *32*, 837−838.
(44) Bain, G. A.; Berry, J. F. *J. Chem. Educ.* **2008**, *85*, 532−536.
(45) Infrared data (cm^{-1}). $K_2[Ni(CN)_4]\cdot xH_2O$: 3640(br), 3565(br), 3546(w), 2120(s), 2084(s), 1621(m), 1599(s), 1381(w); $K_2[Pt(CN)_4]\cdot xH_2O$ (cm^{-1}): 3593(br), 3544(br), 3469(w), 2165(s), 2133(s), 2121(s), 1654(w), 1616(s), 502(m).
(46) (a) Wong-Ng, W.; Culp, J. T.; Chen, Y. S.; Zavalij, P.; Espinal, L.; Siderius, D. W.; Allen, A. J.; Scheins, S.; Matranga, C. *CrystEngComm* **2013**, *15*, 4684−4693. (b) Tao, B.; Xia, H.; Jiang, X.; Zhu, Y. F. *Russ. J. Coord. Chem.* **2011**, *37*, 367−370.
(47) (a) Loosli, A.; Wermuth, M.; Güdel, H. U.; Capelli, S.; Hauser, J.; Bürgi, H. B. *Inorg Chem.* **2000**, *39*, 2289−2293. (b) Mühle, C.; Nuss, J.; Jansen, M. *Z. Kristallogr.* **2009**, *224*, 9−10.
(48) Guionneau, P.; Brigouleix, C.; Barrans, Y.; Goeta, A. E.; Létard, J.-F.; Howard, J. A. K.; Gaultier, J.; Chasseau, D. *C.R. Acad. Sci., Ser. IIc: Chim.* **2001**, *4*, 161−171.
(49) Marchivie, M.; Guionneau, P.; Létard, J.-F.; Chasseau, D. *Acta Crystallogr., Sect. B* **2003**, *59*, 479−486.
(50) (a) Farrugia, L. J. *J. Appl. Crystallogr.* **1997**, *30*, 565. (b) Farrugia, L. J. *J. Appl. Crystallogr.* **2012**, *45*, 849−854.
(51) (a) Shatruk, M.; Dragulescu-Andrasi, A.; Chambers, K. E.; Stoian, S. A.; Bominaar, E. L.; Achim, C.; Dunbar, K. R. *J. Am. Chem. Soc.* **2007**, *129*, 6104−6116. (b) Harris, T. D.; Long, J. R. *Chem. Commun.* **2007**, 1360−1362. (c) Coronado, E.; Gimenez-Lopez, M. C.; Korzeniak, T.; Levchenko, G.; Romero, F. M.; Segura, A.; Garcia-Baonza, V.; Cezar, J. C.; de Groot, F. M. F.; Milner, A.; Paz-Pasternak, M. *J. Am. Chem. Soc.* **2008**, *130*, 15519−15532. (d) Avendano, C.; Karadas, F.; Hilfiger, M.; Shatruk, M.; Dunbar, K. R. *Inorg. Chem.* **2010**, *49*, 583−594. (e) Zueva, E. M.; Ryabikh, E. R.; Kuznetsov, A. M.; Borshch, S. A. *Inorg Chem.* **2011**, *50*, 1905−1913.

dx.doi.org/10.1021/ic401721x | *Inorg. Chem.* 2014, 53, 97−104